Kapil Mamtani[1]
Christian L. da Silveira[2]
Mohammed M. Farid[1]
Kaveh Shahbaz[1,3,*]

Liquid-Liquid Phase Equilibrium of Glycerolysis Precursors: Experimental and Modeling Study

The mutual immiscibility of glycerol and free fatty acids limits glycerolysis, a reaction capable of upgrading waste-derived oils. In the present work, the liquid-liquid phase equilibrium data for the glycerol-water-oleic acid and glycerol-monoolein-oleic acid ternary systems were determined experimentally and compared with predictions of the UNIFAC-LLE and COSMO-SAC models. Monoolein was found to affect the glycerol solubility in oleic acid strongly. None of the models investigated adequately determined phase equilibria for the glycerol-monoolein-oleic acid system. COSMO-SAC predictions showed the best trend for glycerol solubility in the fatty phase. For the glycerol-water-oleic acid system, UNIFAC-LLE predictions were in good agreement with experimental data.

Supporting Information available online

Keywords: Biphasic system, COSMO-SAC model, Glycerolysis, Liquid-liquid phase equilibria, UNIFAC-LLE model

Received: May 17, 2023; *revised:* August 01, 2023; *accepted:* August 31, 2023

DOI: 10.1002/ceat.202300245

1 Introduction

Esterification processes, generally biphasic, are common for producing essential compounds, e.g., monoolein (MO) and diolein (DO), among other essential glycerides of different acids [1]. One valuable reaction is glycerolysis [2], in which glycerol reacts with free fatty acids (FFAs) to produce glycerides (mono-, di-, and triglycerides) of respective FFAs and water as a byproduct. Glycerides of various FFAs are utilized industrially for food and oleo chemical products. Biodiesel is one such oleo chemical industry where glycerides of FFAs are utilized as potential substitute feedstock for vegetable oils [3, 4]. Thus, glycerolysis provides a pathway to upgrading non-edible waste-derived lipids, such as industrial grease (brown/yellow) and vegetable oil refinery rejects, among many others, making glycerolysis a worthy research investigation.

In a glycerolysis reaction, the reactant glycerol (G) contains three hydroxyl groups linked to it and is a hydrophilic molecule [5]. Therefore, it is far less soluble in organic solutions; for example, it is only 4–5 % soluble in typical hydrophobic fats. This poor solubility impedes the process, and unless a catalyst is used, the reaction is slow and requires high temperatures, around 523 K, when glycerol solubility is roughly 45 % [6]. Such poor immiscibility between reactants, glycerol, and FFAs makes the reaction a biphasic affair, only to homogenize at higher temperatures or in the presence of a solvent or catalyst, and most importantly, it makes reactants phase solubility within a biphasic system a necessary consideration [7].

In our previously published review [8] on glycerolysis of oleic acid (OA), the FFA conversion rate is higher initially when the MO yield is also higher, irrespective of the reaction being catalyzed or non-catalyzed. The presence of MO dictating the conversion of OA in the glycerolysis reaction has been recently well established by the work of Gomes et al. [9]. MO, an ester of OA, was found to act as a phase transfer agent, accelerating the reaction. Given the evidence [9], it is intuitive that the glycerolysis biphasic system's reaction kinetics will be impacted by this changing phase behavior, and thus is worthwhile of an investigation.

The reaction rate and selectivity of the desired product can all be improved with a deeper understanding of the process and knowledge of the phase equilibrium in such a system. Moreover, given that liquid-liquid equilibrium (LLE) holds great significance, the accurate description of an LLE system is of utmost importance. One of the key requirements to get good system predictions is the use of precise models. Similar systems have been described by some authors using UNIFAC [10, 11], while others have applied UNIQUAC [12], NRTL [13, 14], and COSMO-SAC [15]. Although the NRTL and UNIQUAC

---

[1] Dr. Kapil Mamtani https://orcid.org/0000-0003-4539-0279, Prof. Mohammed M. Farid, Dr. Kaveh Shahbaz
(k.shahbaz@auckland.ac.nz)
Department of Chemical and Materials Engineering, The University of Auckland, Auckland, AKL 1010, New Zealand.

[2] Prof. Christian L. da Silveira
Chemical Engineering Department, Federal University of Santa Maria, Santa Maria – RS, 97105-900, Brazil.

[3] Dr. Kaveh Shahbaz
Circular Innovations (CIRCUIT) Research Centre, The University of Auckland, Auckland, 1010, New Zealand.

models provide good data correlation, the UNIFAC-LLE model has higher predictive power, as it describes the interaction between functional groups, providing the model with more versatility for data prediction [16, 17].

In the last few decades, the COSMO-SAC model, a highly predictive excess Gibbs energy model, has been successfully used for several thermodynamics properties predictions and equilibrium calculations, including LLE [18, 19]. Thus, these two predictive models, namely, (i) UNIFAC-LLE, requiring binary interaction parameters for every pair of groups in the mixture, which are obtained here from empirical correlations, and (ii) COSMO-SAC, which relies on the ab initio calculation of the molecular electrostatic potential, were used to evaluate ternary tie lines data.

In this study, phase equilibria of the glycerol-monoolein-oleic acid at 343 K and of the glycerol-water-oleic acid at 303 K, 323 K, and 343 K, were experimentally investigated. The experimentally obtained data were compared with predictions by UNIFAC-LLE and COSMO-SAC thermodynamic models.

2 Material and Methods

2.1 Materials

Tab. 1 presents the materials used in this investigation with their necessary specifications. Water (deionized) was available in lab and used without any modifications. For analysis of the glycerol-water-oleic acid system, technical-grade OA was used, while for glycerol-monoolein-oleic acid system analytical-grade OA was taken. The choice of using different grades of OA in the two ternary systems was influenced by the cost of chemicals and a perceived relative sensitivity of glycerol-monoolein-oleic acid ternary system towards impurities in comparison to the other ternary system.

Also, the analysis of the supplied technical-grade OA showed that the overall content of C-18 (C18:0–C18:3) was 98 ± 1 %, of which the OA content was 85 ± 1 %. Thus, the technical-grade OA was found suitable for the LLE investigation of the glycerol-water-oleic acid system. 1-Oleoyl-rac-glycerol and analytical-grade OA were used for preparing standards for gas chromatography (GC) calibration (Fig. S1, Supplementary Information). The water contents of hygroscopic glycerol and technical-grade OA were 0.17 % and 0.12 %, respectively, analyzed via Karl-Fischer titration, a methodology which is discussed in Sect. 2.4. All the chemicals listed in Tab. 1 were used without any modifications.

2.2 Thermodynamic Modeling

2.2.1 UNIFAC-LLE Model

At equilibrium, two liquid phases can be described by Eq. (1):

$$x_i^{\mathrm{I}} \gamma_i^{\mathrm{I}}\left(T, P, \mathbf{x}^{\mathrm{I}}\right) = x_i^{\mathrm{II}} \gamma_i^{\mathrm{II}}\left(T, P, \mathbf{x}^{\mathrm{II}}\right) \tag{1}$$

where x_i and γ_i are the molar fraction and activity coefficients of component i in phase I and vice versa for phase II; T and P are the temperature and pressure of the system; $\mathbf{x}^{\mathbf{I}}$ and $\mathbf{x}^{\mathbf{II}}$ are the vectors of compositions of the phases I and II.

Predictive methods such as UNIFAC [20] can be used to calculate γ_i, when the experimental data is not available. However, as it is well-known that model predictions can sometimes diverge significantly from reality, and experimental data are required to validate model predictions. Such experimental data can also be helpful for estimating the thermodynamic models' missing parameters. UNIFAC details can be found in the literature [16, 20].

Magnussen et al. [17] introduced the UNIFAC parameters for the LLE data prediction. A few issues related to the application of UNIFAC-LLE to the ternary systems examined in this study consist of a narrow recommended temperature range (283–313 K), and when molecules of significantly different sizes are involved, the activity coefficients at infinite dilution are frequently inadequate. The group contributions of molecules [17] present in the examined system according to UNIFAC-LLE are given in Tab. S1 (Supporting Information).

2.2.2 COSMO-SAC Model

The COSMO-SAC model is based on the COSMO (conductor like screening model) theory, presented by Klamt and Schüürmann [21], which considers the solvation energy of a molecule in a perfect conductor. This allows the determination of the chemical potential of any species in a mixture from quantum mechanics calculations [22], making COSMO-SAC an excess

Table 1. Material list with specifications.

Reagent	IUPAC (PIN)	CAS No.	Supplier	Assay
1-Oleoyl-rac-glycerol (monoolein)	2,3-Dihydroxypropyl (Z)-octadec-9-enoate	111-03-5	Sigma-Aldrich	≥ 99 %
Glycerol	Propane-1,2,3-triol	56-81-5	ECP Ltd.	≥ 99.5 %
n-Hexane	Hexane	110-54-3	ECP Ltd.	≥ 99 %
Oleic acid (technical)	(9Z)-Octadec-9-enoic acid	112-80-1	ECP Ltd.	75 %
Oleic acid (analytical)	(9Z)-Octadec-9-enoic acid	112-80-1	Sigma-Aldrich	≥ 99 %
HYDRANAL™ Water Standard 10.0[a]	–	108-32-7	Merck	–

[a] IUPAC (PIN) and assay unavailable.

Gibbs energy model with high predictive capacity. The highly predictive capacity of the COSMO-SAC model arises from a very important feature of the molecule for the model, i.e., the sigma profiles. The sigma profiles are characteristic of each molecule and can be obtained solely by quantum mechanics calculations based on each atom type and position. The relevant computational details are provided in the Supplementary Information. In Fig. 1, the sigma profiles of the four molecules used in this work, namely, glycerol, OA, MO, and water, are depicted.

It can be seen, for instance, that the sigma profile for water has a very low area in the neutral charge density region, having most of its charge densities distributed close to +0.01 and –0.01 e A^{-2}, representing the water capacity of being both hydrogen-bond donor and acceptor. On the other hand, the OA, which is mostly comprised by CH_3 functional groups, has a highly apolar chain, resulting in a large area for neutral charge densities. The glycerol molecule presents both neutral (central alkyl groups) and non-neutral charges (positive, arising from the charges induced by the oxygen, and negative from the charges induced by the hydroxyl group).

The sigma profile for MO shows some small positive induced charges areas, being mostly due to the oxygen in the hydroxyl group, and the carbonyl functional group in the molecule. There are also considerable negative induced charge areas for MO which overlaps the glycerol's negative charge area. Again, like that of glycerol, this can be attributed to arising from the charges induced by the hydrogen in the hydroxyl group. However, most of the MO molecule is composed of hydrocarbyls, which explains the large neutral area shown in Fig. 1 for MO.

Hsieh and co-workers [23] reported a modified version of the COSMO-SAC model which can improve vapor-liquid equilibrium (VLE) and LLE prediction accuracy. In this version, the electrostatic interaction parameter is a temperature-dependent parameter, and the hydrogen-bonding term is divided between hydroxyl group interactions with another hydroxyl group (OH–OH), hydroxyl group with other hydrogen bonding group (OH–OT), and only non-hydroxyl hydrogen bonding groups interacting with each other (OT–OT); where OT represents the other hydrogen bonding/acceptor that is not OH. Hence, in this work, the COSMO-SAC (2010) was used to describe the LLE of the ternary systems.

In essence, first the thermodynamic models UNIFAC-LLE and COSMO-SAC were applied individually to calculate the activity coefficients. Finally, the Rachford-Rice algorithm was used to compute the tie lines of the ternary LLE. The tie lines computational procedure for ternary LLE for both thermodynamic models used is provided in the Supplementary Information.

2.3 Experimental Setup and Procedure

During experimental investigations in a non-catalyzed glycerolysis of OA where the glycerol-to-OA molar ratio was 6:1, at 363 K for 5 h, the conversion was found to be negligible (≤ 1 %). A conservative strategy of investigating phase solubility at lower temperature than 363 K was adopted to avoid any chance of reaction taking place. The two ternary systems were investigated at 303 K, 323 K, and 343 K both via thermodynamic modeling and experimentally. Due to a rather expensive MO, the glycerol-MO-OA ternary system was only experimentally verified at 343 K.

A glass vessel fitted with an IKA EUROSTAR 60 Overhead Stirrer was used to perform the LLE experiments. The glass vessels were heated to the desired temperature by a Grant laboratory heated water bath equipped with GD100 digital controller. The experiments with the glycerol-water-OA system were performed in a 20-mL glass vessel, and the experiments with the glycerol-MO-OA system in a 2-mL glass vessel. The typical procedure, identical in both cases, involved adding two immiscible components (glycerol and OA) into the glass vessel at a specific molar ratio, and the third component (water or MO) was added in steps to obtain phase compositions for different tie lines.

Afterwards, the phases were stirred vigorously using axial stirring to ascertain that well-dispersed conditions were maintained. The stirring at 600 rpm was done for 150 min, a time in which good phase dispersion was achieved. Then, the mixture was allowed to separate until both phases were clear. For the

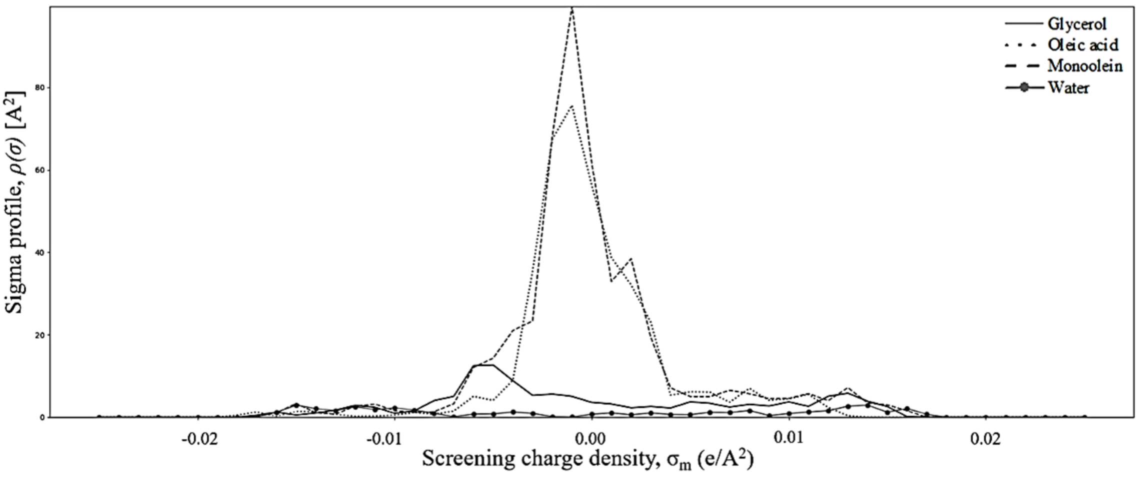

Figure 1. Sigma profiles of glycerol, oleic acid, monoolein, and water.

glycerol-water-OA system, samples of 1.5 mL were withdrawn from both phases systematically with a clean glass syringe equipped with an 18-gauge stainless-steel needle for GC analysis and then for water content analysis. During sample withdrawal, every effort was made to avoid interfering with the phases which became more difficult and important when using a 2-mL glass vessel.

After the samples from the OA phase were withdrawn for OA content analysis using GC, from the same volume, samples were sent for water content analysis. For the glycerol-MO-OA system, samples of 20 µL volume were withdrawn from both phases and sent for GC analysis to ascertain the OA and MO content. In both systems, the glycerol content was then straightforward to calculate once the other two components have been calculated analytically as described above. In the case of the glycerol-water-OA system, no OA was detected in the glycerol phase.

The aforementioned experimental procedure was adapted from the works of Negi et al. [11], with only modifications in GC analysis owing to the difference in instrument specifications used and nature of solute-solvent interactions in the GC instrument.

2.4 Analysis

The water content was measured using a Karl Fischer Moisture Analyzer (T5, Mettler Toledo). The measurement accuracy of the Karl Fisher coulometer was checked with HYDRANAL–water standard (10.00 mg g^{-1}). This standard was supplied in glass ampoules from Merck Pty Limited. For the determination of OA and glycerides content, the analysis was performed using a Shimadzu GC 2010 gas chromatograph equipped with split injection and flame ionization detector (FID). The GC method adopted here has been previously used by Zhang et al. [24] validating the methodology.

Separation occurred on an Agilent capillary DB-1HT column (15 m, 0.25 mm ID, 0.1 µm film thickness). Instrument-grade helium served as carrier gas at a constant flow of 30 mL min^{-1} and the makeup gases consisted of hydrogen and dry air at constant flows of 40 and 400 mL min^{-1}, respectively. Sample volumes of 0.5 µL were injected at 563.15 K with a split ratio of 20:1, while the FID detector was set to 653.15 K. The column oven temperature was programmed as follows: 323.15 K held for 1 min; 373.15 K at 50 K min^{-1}; 493.15 K at 80 K min^{-1}; 563.15 K at 30 K min^{-1}; 603.15 K at 50 K min^{-1} and held 2 min; and 653.15 K at 50 K min^{-1} and held for 3 min.

Linearity was established for standard solutions of OA and MO from 50 to 1000 ppm, and 1 mg mL^{-1} solutions of the product were taken from the upper layer using *n*-hexane as the solvent. The solution was then filtered through a 0.22-µm PTFE filter and vialed for GC analysis. The determination of a fatty acid and its glycerides is dependent on the interactions between internal column materials with the specific glycerides. Analysis was done on duplicates.

The mass of component *i* in the injected sample, w_i, is proportional to the area, A_i, of the GC peak:

$$w_i \propto f_i A_i \tag{2}$$

where f_i is the response factor of component *i* as obtained by calibration.

The mole fraction (x) of component *i* in the injected sample can be calculated as:

$$x_i = (w_i/M_i)/\sum(w_i/M_i) \tag{3}$$

where M_i is the molecular weight of component *i*. For the doublets analyzed for all the samples taken from each phase, the standard deviations were under 10 %, and very good calibrations for GC-FID were achieved for OA (R^2 0.998) and MO (R^2 0.999). For water content analysis, the maximum standard deviations were under 5 %.

Additionally, the root-mean-square error (Δx_{RMS}) was also evaluated for both the models to explore the extent of deviations. The root-mean-square error between the experimental and predicted tie lines in ternary diagrams [15] is defined as per Eq. (4):

$$\Delta x_{\mathrm{RMS}} = \sqrt{\sum_{\mathrm{nT}} \sum_{\mathrm{nP}} \sum_{\mathrm{nC}} \frac{(x_{\mathrm{P}} - x_{\mathrm{E}})^2}{(nT \cdot nP \cdot nC)}} \tag{4}$$

where x_{P} is the predicted mole fraction, x_{E} is the experimental value of the mole fraction, nT denotes the number of tie lines, nP the number of phases ($nP = 2$), and nC the number of components ($nC = 3$).

3 Results and Discussion

3.1 Glycerol-Monoolein-Oleic Acid System

The experimental data and computed component mole fractions for the two phases at equilibrium at 343 K, in addition to the tie lines computed from UNIFAC-LLE and COSMO-SAC models, are depicted in Fig. 2. The effect of MO on the glycerol solubility in the fatty phase was observed to be significant and desirable. On the contrary, the lipid solubility in the glycerol phase is negligible. It was interesting to observe that when the MO-to-OA molar ratio is 0.5, no glycerol was detected in the fatty phase, marking the lower limit for the MO-to-OA molar ratio for having any increase in glycerol solubility in the fatty phase. As the MO-to-OA molar ratio increases, the glycerol solubility rises in proportion. For equimolar MO and OA in the feed composition, glycerol solubility was observed to be approximately 43 %. For higher MO-to-OA molar ratios in the feed composition, the glycerol solubility in the fatty phase further increments to 57 % and 60 %.

Moving on the model predictions, the predictions based on the two models for the glycerol phase are in a good agreement with the experimental data to some extent, showing significantly less solubility for MO and OA in the glycerol phase. Both model predictions can only be treated as qualitatively correct for the fatty phase, given both models forecast an increase in glycerol solubility in OA on the addition of MO. The solubility of glycerol in the fatty phase was predicted to be substantially lower by UNIFAC-LLE. COSMO-SAC predictions for the fatty phase showed the best trend. This suggests that the inter-

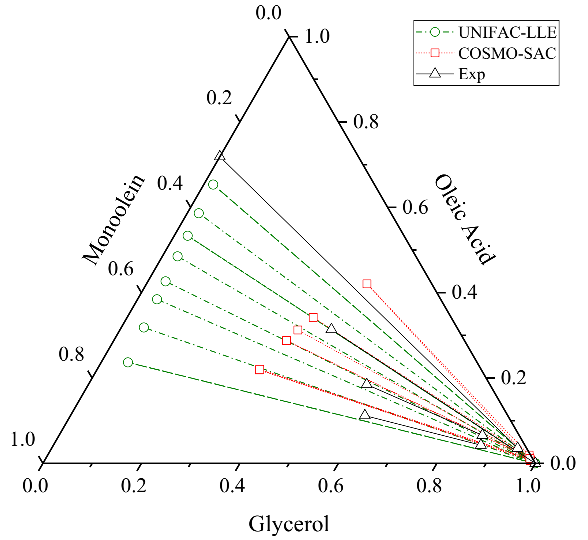

Figure 2. Ternary diagram for glycerol-monoolein-oleic acid at 343 K (± 3 K). Comparison of experimental data (black solid lines with triangle symbol) with UNIFAC-LLE (green dashed lines with circle symbol) and COSMO-SAC (red dashed lines with square symbols) models.

action parameters adopted in this study need more optimization in case of the UNIFAC-LLE model. For COSMO-SAC used in this study (see Supporting Information), even though different types of H-bonding for a molecule were considered to improve the accuracy of LLE predictions, it is still not satisfactory yielding only qualitative results. This opens up the scope for further optimization in the present COSMO-SAC model.

Both of the models' predictions were similar at 303 K, 323 K, and 343 K, hence model predictions at lower temperatures was not mentioned here. The tie line data are provided in Tab. 2. The root mean square (RMS) errors evaluated for COSMO-SAC and UNIFAC-LLE thermodynamic models, were 15.97 % and 23.34 %, respectively.

Table 2. Compositions of the points on the tie lines in the ternary diagram for glycerol-monoolein-oleic acid at 343 K (± 3 K).

Glycerol phase			Fatty phase		
x'_{G}	x'_{MO}	x'_{OA}	x''_{G}	x''_{MO}	x''_{OA}
0.95	0.02	0.04	0.00[a]	0.28	0.72
0.87	0.09	0.04	0.60	0.29	0.11
1.00	0.00	0.00[b]	0.43	0.26	0.31
0.89	0.04	0.04	0.57	0.25	0.18

[a] The ratio of oleic acid to monoolein mole fraction in the feed was much lower. [b] No oleic acid was detected in GC analysis.

3.2 Glycerol-Water-Oleic Acid System

Fig. 3 presents the experimental data for the glycerol-water-OA system at three temperatures investigated during the LLE study. It is observed that the tie lines for the three temperatures overlap each other. The tie line data is provided in Tab. 3. The glycerol solubility in the fatty phase and OA solubility in the glycerol phase were both negligible with changing the water-to-OA molar ratios. This suggests that water does not influence any change in glycerol and OA mutual solubility, as observed with MO.

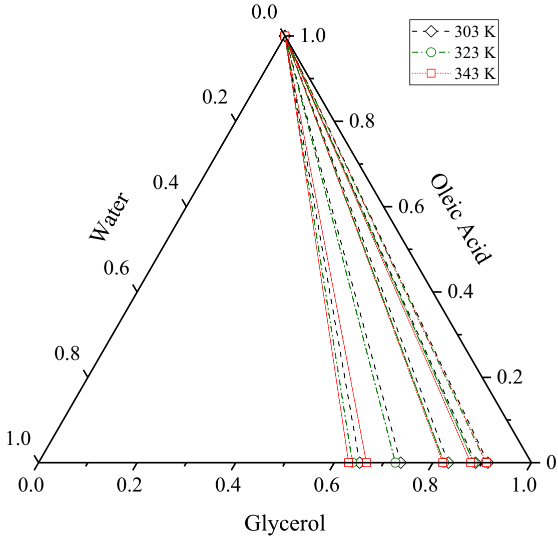

Figure 3. Experimental data-based ternary diagram for glycerol-water-oleic acid at 303 K (± 3 K) (black dashed lines with rhombus symbol), 323 K (± 3 K) (green dashed lines with circle symbol), and 343 K (± 3 K) (red dashed lines with square symbol).

Table 3. Compositions of the points on the tie lines in the ternary diagram for glycerol-water-oleic acid at 343 K (± 3 K).

Glycerol phase			Fatty phase		
x'_{G}	x''_{H2O}	x'_{OA}	x''_{G}	x''_{H2O}	x''_{OA}
0.91	0.09	0.00[a]	0.0020	0.0010	0.9970
0.88	0.12	0.00[a]	0.0020	0.0015	0.9965
0.82	0.18	0.00[a]	0.0025	0.0020	0.9955
0.67	0.33	0.00[a]	0.0020	0.0040	0.9940
0.63	0.37	0.00[a]	0.0020	0.0050	0.9930

[a] No oleic acid was detected in GC analysis.

A similar trend was observed in predictions for both UNIFAC-LLE and COSMO-SAC models, where tie lines overlapped each other for all three temperatures. These results demonstrate that within the examined range the temperature has a negligible impact on the mutual solubility of glycerol-OA. A comparison of the experimental data and predictions based on UNIFAC-LLE and COSMO-SAC is displayed in Fig. 4.

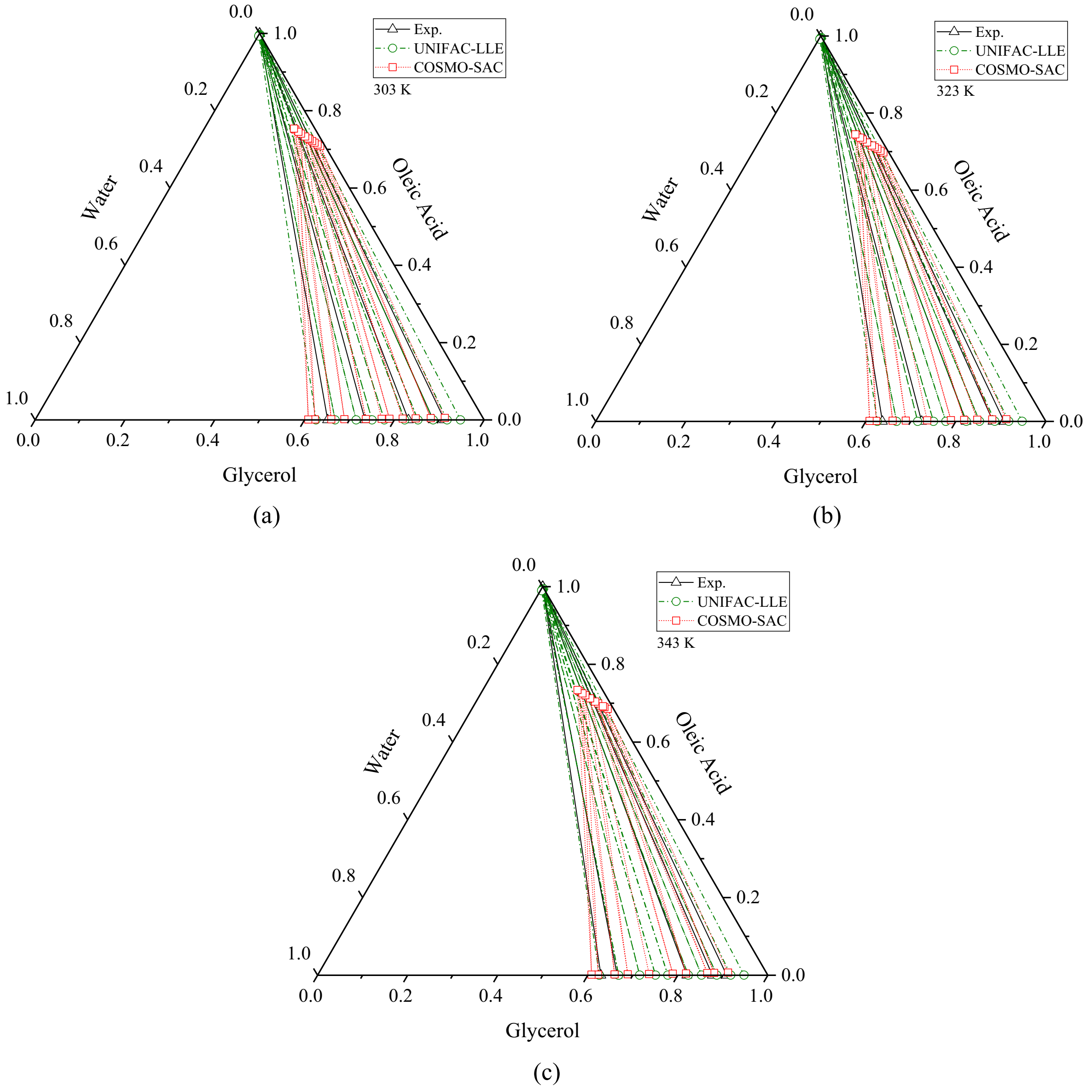

(a)

(b)

(c)

Figure 4. Ternary diagram for glycerol-water-oleic acid system at: (a) 303 K (± 3 K), (b) 323 K (± 3 K), and (c) 343 K (± 3 K). Comparison of experimental data (black solid lines with triangle symbol) with UNIFAC-LLE (green dashed lines with circle symbol) and COSMO-SAC (red dashed lines with square symbols) models.

UNIFAC-LLE predictions for glycerol phase and fatty phase are in good agreement with experimental data, whereas for COSMO-SAC a much greater glycerol solubility in the fatty phase is predicted, similar to the glycerol-MO-OA system as before. The RMS error evaluated for COSMO-SAC and UNIFAC-LLE thermodynamic models were 15.24 % and 1.55 %, respectively. The good predictions by the UNIFAC-LLE model for this ternary system indicate that for a less complex molecule, i.e., water, the interaction (group contribution) parameters adopted were optimized. However, this was not the case in the MO-based ternary system in Sect. 3.1. As for COSMO-SAC, the overpredictions for glycerol solubility in the fatty phase suggest similar solution to Sect. 3.1. i.e., further optimize the model.

3.3 Tie Line Correlation

Tie line correlation, as equated below and introduced by Othmer and Tobias [25], can be used to evaluate the validity of experimental results in a ternary system at LLE.

$$\log\left(\frac{1-a}{a}\right) = n \cdot \log\left(\frac{1-b}{b}\right) + S \tag{5}$$

where a is the mole fraction of the solvent in the solvent phase and b is the mole fraction of the diluent in the conjugate phase.

As can be seen in Figs. 5 and 6, the experimentally acquired data for the two ternary systems provide a good linear fit with

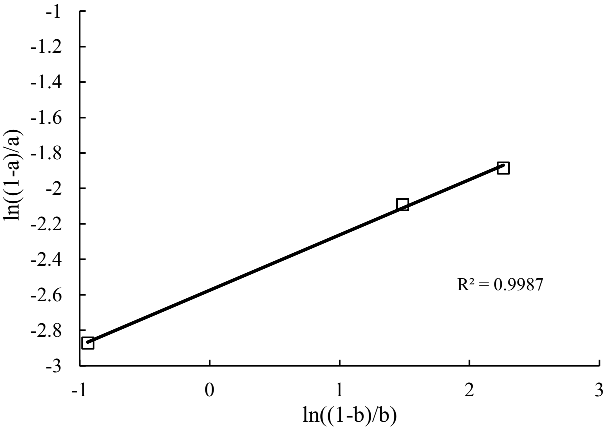

Figure 5. Othmer-Tobias plot for the experimental data from the glycerol-monoolein-oleic acid system at 343 K, where *a* is the mole fraction of glycerol in the glycerol phase and *b* is the mole fraction of oleic acid in the fatty phase.

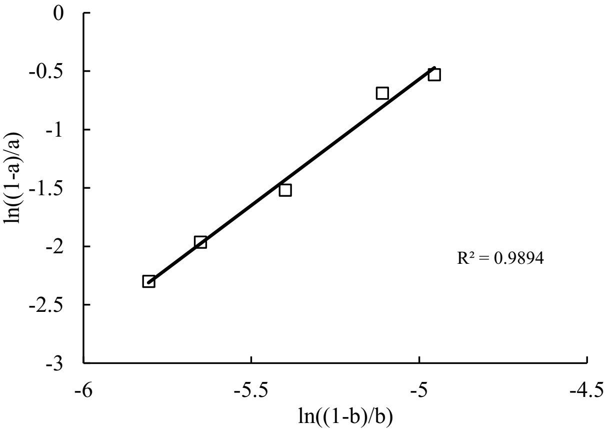

Figure 6. Othmer-Tobias plot for the experimental data from the glycerol-water-oleic acid system at 343 K, where *a* is the mole fraction of glycerol in the glycerol phase and *b* is the mole fraction of oleic acid in the fatty phase.

the tie line correlation, indicating the consistency of the experimental results.

Furthermore, the deviation of slope (*n*) from unity (i.e., lines are not at 45°), suggests that the systems investigated are not completely immiscible. The reason for this variation in the slope is attributed to the formation of either associated or dissociated molecules in the solution [25]. Referring to Fig. 1, it was previously mentioned that in the sigma profiles the small negative induced charge areas of glycerol were exactly overlapped by negative induced charge areas for MO.

Upholding the above two empirical evidences, it can be concluded that the mutual presence of hydroxyl groups in glycerol and MO in the present investigated system might promote the formation of an associated or dissociated complex between these species, favoring the glycerol solubility in the fatty phase. This justification is in agreement with the results of Gomes et al. [10], where the authors attributed MO to behave as a phase transfer agent, which necessarily aims towards the formation of associated or dissociated molecules in the solution.

4 Conclusion

An LLE study was conducted for two nearly immiscible glycerol and fatty phases to investigate the effects of the third component, MO and water, both being the products in the glycerolysis of OA. LLE phase solubility was explored via thermodynamic models, namely, UNIFAC-LLE and COSMO-SAC, as well as experimentally. Model predictions for the glycerol-MO-OA system were only qualitatively accurate with COSMO-SAC showing the best trend whereas UNIFAC-LLE was found inadequate. Predictions for the glycerol-water-OA system were in good agreement with experimental data for the UNIFAC-LLE model whereas COSMO-SAC overpredicted the glycerol solubility in the fatty phase. Phase predictions for both models were not very accurate, especially in the fatty phase, suggesting that more work on model parameter optimization is required for the present ternary systems investigated.

The results for the glycerol-MO-OA system suggest that the presence of MO in the biphasic immiscible system increases the glycerol solubility in the fatty phase, even though the mutual solubility of glycerol and OA does not much change in the temperature range studied. The increased glycerol solubility in the fatty phase, dictated by the MO concentration, also opens up the scope of process intensification for glycerolysis reaction by introducing MO at the beginning of the reaction.

Supporting Information

Supporting Information for this article can be found under DOI: https://doi.org/10.1002/ceat.202300245. This section includes additional references to primary literature relevant for this research [26–28].

The authors have declared no conflict of interest.

Acknowledgment

The authors acknowledge the New Zealand Government through the Ministry of Foreign Affairs and Trade (MFAT) for providing New Zealand Development Scholarships. The Coordination for the Improvement of Higher Education Personnel (CAPES) and its internationalization program (PrInt) of the Brazilian Ministry of Education (MEC) is gratefully acknowledged for financially supporting Prof. Christian Silveira's participation in this work. We also acknowledge Raymond Hoffmann (Senior Technician), Chemical and Materials Engineering Department, The University of Auckland, for his support with fabrication of glass vessels necessary for the LLE study. Open access publishing is facilitated by The University of Auckland, as part of the Wiley – The University of Auckland agreement via the Council of Australian University Librarians.

Symbols used

f	[–]	calibration-based response factor
M	[g mol^{-1}]	molecular weight
P	[bar]	pressure of the system
T	[K]	temperature of the system
w	[g]	mass of any component in the injected sample
x	[–]	molar fraction of a component
$\boldsymbol{x}$	[–]	vector compositions in any phases
y	[–]	activity coefficient of a component

Greek letters

$\rho(\sigma)$	[A^2]	sigma profile
σ_m	[e A^{-2}]	screening charge density

Sub- and superscripts

i	a component in the mixture
I, II	phases I and II in a biphasic system
$'$, $''$	glycerol phase / fatty phase

Abbreviations

FFA	free fatty acid
LLE	liquid-liquid equilibrium
MO	monoolein
OA	oleic acid

References

[1] F. Shahidi, *Bailey's Industrial Oil and Fat Products*, 6th ed., John Wiley and Sons, Newfoundland, Canada **2005**. DOI: https://doi.org/10.1002/047167849X

[2] P. Felizardo, J. Machado, D. Vergueiro, Study on the glycerolysis reaction of high free fatty acid oils for use as biodiesel feedstock, *Fuel Process. Technol.* **2011**, *92 (6)*, 1225–1229. DOI: https://doi.org/10.1016/j.fuproc.2011.01.020

[3] A. Murugesan, C. Umarani, T. R. Chinnusamy, Production and analysis of biodiesel from non-edible oils – A review, *Renewable Sustainable Energy Rev.* **2009**, *13 (4)*, 825–834. DOI: https://doi.org/10.1016/j.rser.2008.02.003

[4] P. D. Patil, S. Deng, Optimization of biodiesel production from edible and non-edible vegetable oils, *Fuel* **2009**, *88 (7)*, 1302–1306. DOI: https://doi.org/10.1016/j.fuel.2009.01.016

[5] R. Christoph, B. Schmidt, U. Steinberner, in *Ullmann's Encyclopedia of Industrial Chemistry*, Wiley-VCH, Weinheim **2006**. DOI: https://doi.org/10.1002/14356007.a12_477.pub2

[6] L. Marrone, L. Pasco, D. Moscatelli, S. Gelosa, Liquid-liquid Phase Equilibrium in Glycerol-methanol-fatty Acids Systems, *Chem. Eng. Trans.* **2007**, 629–634.

[7] L. Zhanenova, S. Behzadi, M. M. Farid, Improving the economics of biodiesel production through esterification of free fatty acid with waste glycerol, in *Engineering our Future: Are we up to the Challenge?* Engineers Australia, Barton, ACT, **2009**.

[8] K. Mamtani, K. Shahbaz, M. M. Farid, Glycerolysis of free fatty acids: A review, *Renewable Sustainable Energy Rev.* **2021**, *137*, 110501. DOI: https://doi.org/10.1016/j.rser.2020.110501

[9] M. de S. Gomes, M. R. D. Santos, A. B. Salviano, F. G. Mendonca, Biphasic reaction of glycerol and oleic acid: Byproducts formation and phase transfer autocatalytic effect, *Catal. Today* **2020**, *344*, 227–233. DOI: https://doi.org/10.1016/j.cattod.2019.02.011

[10] A. Casas, M. J. Ramos, Á. Pérez, Product Separation after Chemical Interesterification of Vegetable Oils with Methyl Acetate. Part II: Liquid-Liquid Equilibrium, *Ind. Eng. Chem. Res.* **2012**, *51 (30)*, 10201–10206. DOI: https://doi.org/10.1021/ie300791g

[11] D. S. Negi, F. Sobotka, T. Kimmel, G. Wozny, R. Schomacker, Liquid-Liquid Phase Equilibrium in Glycerol-Methanol-Methyl Oleate and Glycerol-Monoolein-Methyl Oleate Ternary Systems, *Ind. Eng. Chem. Res.* **2006**, *45 (10)*, 3693–3696. DOI: https://doi.org/10.1021/ie051271r

[12] L.-H. Cheng, Y.-F. Cheng, S.-Y. Yen, Application of UNIQUAC and SVM to ultrafiltration for modeling ternary mixtures of oil, FAME and methanol, *Chem. Eng. Sci.* **2009**, *64 (24)*, 5093–5103. DOI: https://doi.org/10.1016/j.ces.2009.08.017

[13] E. G. de Azevedo Rocha et al., Liquid-liquid equilibria for ternary systems containing ethylic palm oil biodiesel+ethanol+glycerol/water: Experimental data at 298.15 and 323.15 K and thermodynamic modeling, *Fuel* **2014**, *128*, 356–365. DOI: https://doi.org/10.1016/j.fuel.2014.01.074

[14] C. P. Trentini, N. Postaue, L. Cardozo-Filho, Production of esters from grease trap waste lipids under supercritical conditions: Effect of water addition on ethanol, *J. Supercrit. Fluids* **2019**, *147*, 9–16. DOI: https://doi.org/10.1016/j.supflu.2019.02.008

[15] M. R. Shah, G. D. Yadav, Prediction of Liquid-Liquid Equilibria for Biofuel Applications by Quantum Chemical Calculations Using the Cosmo-SAC Method, *Ind. Eng. Chem. Res.* **2011**, *50 (23)*, 13066–13075. DOI: https://doi.org/10.1021/ie201454m

[16] A. Fredenslund, R. L. Jones, J. M. Prausnitz, Group-contribution estimation of activity coefficients in nonideal liquid mixtures, *AIChE J.* **1975**, *21 (6)*, 1086–1099. DOI: https://doi.org/10.1021/ie201454m

[17] T. Magnussen, P. Rasmussen, A. Fredenslund, UNIFAC parameter table for prediction of liquid-liquid equilibriums, *Ind. Eng. Chem. Process Des. Dev.* **1981**, *20 (2)*, 331–339. DOI: https://doi.org/10.1021/i200013a024

[18] S.-T. Lin, J. Chang, S. Wang, W. A. Goddard, S. I. Sandler, Prediction of Vapor Pressures and Enthalpies of Vaporization Using a COSMO Solvation Model, *J. Phys. Chem. A* **2004**, *108 (36)*, 7429–7439. DOI: https://doi.org/10.1021/jp048813n

[19] C. L. da Silveira, N. P. G. Salau, The UNIFAC-LLE and COSMO-SAC ternary aqueous LLE calculations, *Fluid Phase Equilib.* **2019**, *501*, 112278. DOI: https://doi.org/10.1016/j.fluid.2019.112278

[20] J. Gaube, A. Fredenslund, J. Gmehling, P. Rasmussen, Vapor-liquid equilibria using UNIFAC a group-contribution method, *Ber. Bunsen Ges. Phys. Chem.* **1978**, *82 (5)*, 551. DOI: https://doi.org/10.1002/bbpc.197800104

[21] A. Klamt, G. Schüürmann, COSMO: a new approach to dielectric screening in solvents with explicit expressions for the screening energy and its gradient, *J. Chem. Soc.* **1993**, *5*, 799–805. DOI: https://doi.org/10.1039/P29930000799

[22] S.-T. Lin, S. I. Sandler, A Priori Phase Equilibrium Prediction from a Segment Contribution Solvation Model, *Ind. Eng. Chem. Res.* **2002**, *41 (5)*, 899–913.

[23] C.-M. Hsieh, S. I. Sandler, S.-T. Lin, Improvements of COSMO-SAC for vapor-liquid and liquid-liquid equilibrium predictions, *Fluid Phase Equilib.* **2010**, *297 (1)*, 90–97. DOI: https://doi.org/10.1016/j.fluid.2010.06.011

[24] T. Zhang, K. Shahbaz, M. M. Farid, Glycerolysis of free fatty acid in vegetable oil deodorizer distillate catalyzed by phosphonium-based deep eutectic solvent, *Renewable Energy* **2020**, *160*, 363–373. DOI: https://doi.org/10.1016/j.renene.2020.07.026

[25] D. Othmer, P. Tobias, Liquid-Liquid Extraction Data - The Line Correlation, *Ind. Eng. Chem.* **1942**, *34 (6)*, 693–696. DOI: https://doi.org/10.1021/ie50390a600

[26] R. Xiong, S. I. Sandler, R. I. Burnett, *Ind. Eng. Chem. Res.* **2014**, *53 (19)*, 8265–8278.

[27] I. H. Bell, *J. Chem. Theory Comput.* **2020**, *16 (4)*, 2635–2646.

[28] J. P. O'Connell, J. M. Haile, *Thermodynamics: Fundamentals for Applications*, Cambridge University Press, Cambridge **2005**.